



# Numerical Study of Individuals Exposure to Road-Noise in Urban Environments

Amin Nabikhani<sup>(✉)</sup>, Tobias Simon Müller, and Arne Henning

German Aerospace Center (DLR), Institute of Aerodynamics and Flow Technology,  
Bunsenstr. 10, 37073 Göttingen, Germany  
[amin.nabikhani@dlr.de](mailto:amin.nabikhani@dlr.de)

**Abstract.** In this paper a method is presented, which allows to simulate the traffic noise exposure of people living in an urban area. This is in contrast to classical noise maps, where the noise exposure of locations is calculated. A temporally resolved noise mapping is used in combination with an agent model, which simulates the location of persons in an urban area. Noise exposure is then assigned to agents based on their specific locations throughout the day, and averaged over time. The question is answered what difference in noise exposure the method shows in comparison to classical noise-maps. The method was successfully applied for a part of Berlin. It is shown that the average noise to which the agents are exposed during the day is increased due to their motion. This is not always due to the fact that people spend more time in places with high noise exposure. Rather, the usual consideration of the noise exposure in a log scale is responsible for this. This always results in a dominance of the noisier locations in the daily mean of the considered agents. It is to be discussed whether this shift towards higher noise exposure corresponds to the actual subjective perception of persons.

## 1 Introduction

The adverse impact of environmental noise on individuals are of interest to many medical and behavioral studies addressing insomnia, cognitive performance and even cardiovascular diseases. Civil noise caused particularly by transportation means are among the most significant sources. According to an estimation of the World Health Organization (WHO), at least one million healthy disability-adjusted life-years (DALYs) are lost annually due to environmental noise [1]. An accurate method for simulating the exposure of individuals to road-noise during a typical working day in urban environments can help to investigate the physiological impact of noise pollution on the population. It can also be used as an efficient means for planning urban environments with optimal balance between traffic flow efficiency and noise pollution. Studies in the past have shown that if the individual mobility of people is ignored, there may be errors in the calculation of the actual exposure to environmental effects like noise. The effect associated with ignoring these effects are called the neighborhood effect averaging problem (NEAP) [2]. Research in the past has investigated these effects by

means of tracking individuals using personal noise dosimeters [3,4] or combining mobility data sets with pollution maps [5,6]. The present work combines three state-of-the-art simulation tools in order to provide an accurate account for the noise level perceived by a portion of the inhabitants of Berlin during a typical working day. Our study explores the impact of mobility on the exposure to environmental noise explicitly. The first tool in the simulation chain is the Travel Activity Pattern Simulation (TAPAS) which determines the traffic demand on the basis of a synthetic population of individuals [7]. This synthetic population is divided into different socio-economic and socio-demographic groups and daily activity plans are constructed for each individual. It is worth mentioning that the activity plans are not constructed randomly, but they are based on 35.000 diaries of 12.600 people who participated in a survey of the Federal Statistical Office of Germany in 2001/2002. After the traffic demand has been determined by TAPAS in form of origin, destination and arrival time for each individual, the second stage is the microscopic simulation of the traffic flow using SUMO (Simulation of Urban Mobility) [8]. As input to SUMO the true-to-scale road network and the corresponding schedules of the traffic-light systems are provided for the considered region in the center of Berlin. On the basis of this data SUMO simulates the traffic flow in the considered region during a full day. The output of SUMO is composed of the trajectories of all vehicles inside the considered region with a temporal resolution of one second. The last step in the simulation chain is the generation of a time-resolved noise map, which will be described in the following section in more detail. Finally, the resulting time-resolved noise map is combined with the results of TAPAS in order to generate a personal noise diary for every individual in the simulated population.

## 2 Generation of Time-Resolved Noise Maps

In order to evaluate the noise exposure of each individual in the simulated population, a time-resolved noise map is generated which covers a time frame of 24h for a complete district of Berlin city. The generation of this time-resolved noise map is based on the CNOSSOS-EU guideline [9] and is divided into a three-step process which is described in the following.

### 2.1 Geometry Processing

In a first step the relevant geometries are parsed, which includes the road network and the buildings inside the district. The corresponding data are provided respectively in form of a SUMO network [8] by the department of “Design & Bewertung von Mobilitätslösungen” of the DLR in Braunschweig and in CityGML format by the “Senate Department for Urban Development and Housing”. The buildings are represented in LOD1, i.e., they are described by a 2D polygonal outline which is extruded to the buildings height. After the road network has been parsed, static emitter points with a mutual distance of 2 m are placed along the individual lanes [see Fig. 1(a)]. Similarly, static receiver points are placed

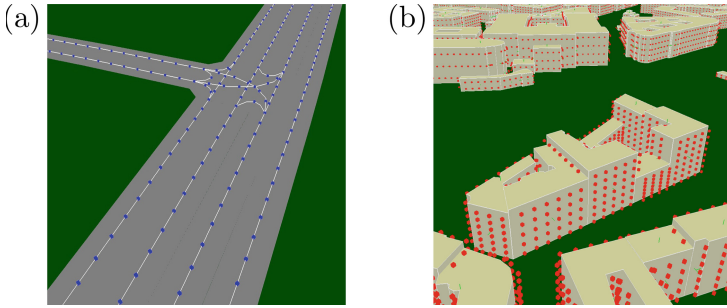


**Fig. 1.** (a) Static emitter points (blue) placed along the individual lanes of the road network. (b) Static receiver points (red) placed in front of building façades. (Color figure online)

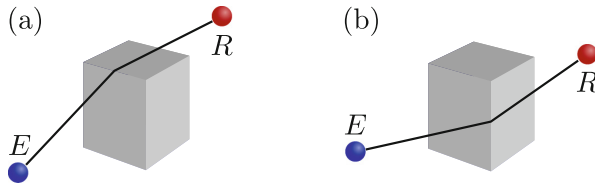


**Fig. 2.** The two kinds of diffraction patterns considered during the construction of the rays between an emitter  $E$  and a receiver  $R$ : (a) diffraction on the horizontal edges of obstacles and (b) “lateral” diffraction on the vertical edges of obstacles.

4 m above the ground on a regular grid covering the complete district. Static receiver points are also placed 2 m in front of building façades [see Fig. 1(b)]. As described in more detail later, the static emitter and receiver points are used as an approximation for the location of individual vehicles (emitters) and agents (receivers) respectively. Using static emitters and receivers allows us to precompute the rays connecting individual pairs of emitters and receivers in the ray-tracing phase (see Sect. 2.2), which can then be used to generate noise maps for arbitrary many traffic scenarios on the given geometry.

### 2.2 Ray Tracing

In the second step we search for rays which connect individual pairs of emitters and receivers. To this aim four different types of rays are considered, which are defined in the CNOSSOS-EU directive [9]. The most important difference between these ray types is the diffraction pattern considered. Type 1 and 2 rays allow for diffractions on the horizontal edges of buildings [see Fig. 2(a)], while Type 3 and 4 rays allow for diffractions on vertical edges [see Fig. 2(b)]. The difference between Type 1 and 2 rays and Type 3 and 4 rays respectively is that the former (Type 1 and 3) allow for diffractions only while the latter (Type 2 and 4) may include reflections on the building façades. Due to the different

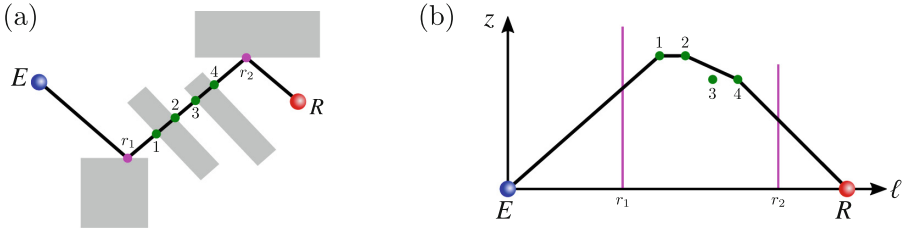


**Fig. 3.** (a) Top-down view of a Type-2 ray between an emitter  $E$  and a receiver  $R$ . The ray contains two reflections,  $r_1$  and  $r_2$ , and intersects building edges at the points 1–4. (b) Construction of the ray profile in the vertical view obtained by “unfolding” the ray at the reflections. The two reflections  $r_1$  and  $r_2$  are indicated by vertical lines having the height of the building on which the respective reflection takes place. Furthermore the points 1–4 mark the locations of the roof edges where intersections have been observed in the top-down view of the ray.

nature of the diffractions involved, the procedure of constructing Type 1 and 2 rays differs to some extent from the one for Type 3 and 4 rays. Type 1 and 2 rays are constructed by using the image-source method in order to obtain a top-down view of all possible rays connecting an emitter to a given receiver by a series of reflections. These rays are permitted to intersect building edges in the top-down view, since the corresponding intersection points are candidates for horizontal diffractions at the roof edges. An example for such a top-down view of a single ray connecting an emitter  $E$  to a receiver  $R$  is shown in Fig. 3(a). In order to obtain the profile of the ray one constructs a vertical plane along each segment of the ray and one “unfolds” these planes at the reflection points like a Chinese screen. In the thus constructed “unfolded” vertical scheme reflections are marked by vertical lines having the height of the building the reflection takes place, and the locations of the roof-edge intersections encountered in the top-down view of the ray are marked by single points [see Fig. 3(b)]. The profile of the ray is then obtained by constructing the convex hull of the emitter, receiver and the roof-edge intersection points. Finally, the ray is validated by checking whether the ray intersects all vertical lines which mark the reflections. A simple example for this procedure is provided in Fig. 3. In order to construct Type 3 and 4 rays one first constructs the propagation plane, which is a tilted horizontal plane<sup>1</sup> containing receiver and emitter. The intersection of the propagation plane with the building outlines yields a 2D geometry in which the actual rays are constructed by an adaptation of the image-source methods which is able to incorporate diffractions at corners of the 2D building outlines. In both methods used for the ray construction the number of permitted reflections and lateral diffractions must be limited. The present results are obtained by allowing for a single reflection and up to four lateral diffractions. Furthermore we have not considered rays whose path length exceeds 350 m. The final step in the ray-tracing

<sup>1</sup> By this we mean that one of the two vectors defining the plane is perpendicular to the  $z$ -direction.

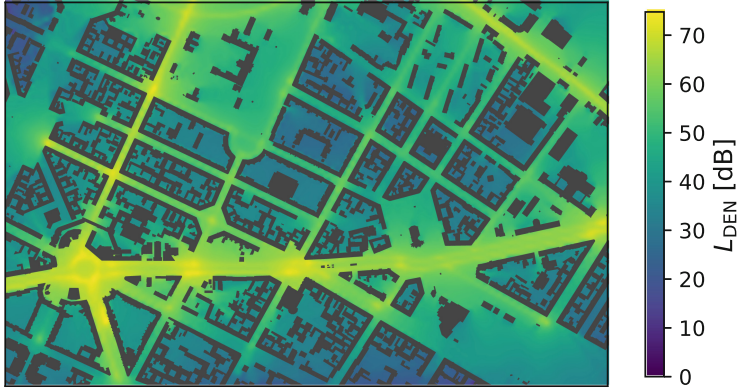


**Fig. 4.** Day-evening-night sound-pressure level  $L_{\text{DEN}}$  for a portion of Berlin Kreuzberg obtained from a time-resolved noise map which covers a full representative day.

algorithm is to compute the attenuation  $A$  of noise during its propagation along the individual rays. The attenuation rules used in the present implementation are described in detail in Sec. VI.4 of the CNOSSOS-EU directive [9].

### 2.3 Noise Calculation

The final step in the process is to determine the actual time-resolved sound-pressure level at the individual receiver points. To this aim we first parse the time-resolved traffic data, which are generated by means of a SUMO simulation [8] and are provided to us by the department of “Design & Bewertung von Mobilitätslösungen” of the DLR in Braunschweig. This data contains the type (passenger car, delivery van, etc.) of each vehicle present in the scene at a given time step, along with its location and velocity. Using these data one computes the sound-power emission  $L(t, f_k)$  for the individual vehicles at each time step  $t$  and for all center frequencies  $f_k$  of the eight octave bands ranging from 125 Hz to 4 kHz, as described in detail in Sect. III.2 of the CNOSSOS-EU directive [9]. This sound power is then distributed across the two emitters which encompass the vehicles position on the lane it is driving on. In order to account for the position of the vehicle relative to these two emitters the sound-pressure level  $L_i(t, f_k) = w_i L(t, f_k)$  ascribed to emitter  $i = 1, 2$  is weighted by  $w_i = 1 - s_i / (s_1 + s_2)$ , where  $s_i$  is the distance between emitter  $i$  and the vehicles momentary position. Subsequently, we use the precomputed rays and propagate the noise from the emitters to the receivers. Let  $R_j$  be one of the receivers which is connected by a given ray to the emitter  $E_i$ . Assume that emitter  $E_i$  emits a total sound power  $L_i(t, f_k)$  at time  $t$ , then the contribution

$$\Delta p_j(t + \ell/c) = \sum_{k=1}^8 10^{A_k/20} p_i(t, f_k) \quad (1)$$

is added to the sound-pressure  $p_j$  perceived at time  $t + \ell/c$  at the receiver location  $R_j$ . Here  $c$  is the speed of sound and  $A_k$  is the attenuation for a sound wave with frequency  $f_k$  propagating along the ray which has a total path length  $\ell$ . Summing all contributions  $\Delta p_j(t)$  given in Eq. (1) for a given time  $t$  yields the time-resolved sound-pressure level  $L_j(t) = 20 \lg[p_j(t)/p_0]$  at the receiver site  $R_j$ . As an example, Fig. 4 shows the day-evening-night sound-pressure level  $L_{\text{DEN}}$  computed from the time-resolved noise-pressure level for a portion of Berlin Kreuzberg. The data used to generate this figure cover a full day with traffic conditions that are representative for an average day within this region.

### 3 Implementation

The demand simulation program TAPAS simulates the daily routines of the individual agents, from which the input data for the traffic simulation SUMO are generated. These included, whereabouts, travel times and choice of transport mode. It is therefore possible to calculate the noise exposure of the respective agents depending on their whereabouts. The starting points and destinations of the agents' trips are available as coordinates. These are assigned to individual buildings for which façade levels are available for coupling to the city's noise map. Before noise diaries are created, a specific façade immission location is assigned for each individual agent, at each of its locations. This is done by random selection. Each location is assigned a building, which in turn is assigned a number of facade immission locations. From these, an immission point is selected by drawing a random number. This assignment remains valid throughout the day. For example, for the time from midnight until the first time one leaves one's home, the same immission point is important as for the time from the last time one enters one's home until the end of the day. The random selection is due to a lack of information. Since there can be several apartments in a building, it is not known from the available data in which part of the building an agent lives. By randomly selecting the immission locations, the influence of this missing information should be kept small. In order to be able to make statements about the whole day, only agents can be considered which have their residence in this area and do not leave the area within the simulated day. For each of the scenarios discussed here, the daily schedules of 3,168,181 agents were created. Of these agents, 88,099 reside within the area. 15,320 of these agents do not leave the area. The agents that do not leave the area visit a total of 18,906 different locations. 18,192 of these locations are indoors. Of the eligible agents, 2,782 visit locations that are not in buildings and are therefore excluded. This leaves 12,538 included agents.

Two energy-equivalent average levels from two different level time courses are determined for each agent. One average level is determined at the facade immission point of the dwelling. The second one results from the level time course considering the different residence locations. Since the locations are given with a temporal resolution of one minute, the level time histories are also formed from levels averaged over one minute. A temporal weighting is omitted for the

time being. If the energetic average over time is formed for each agent, a pair of values of energy-equivalent averaging levels results in each case. In the following, the average level at the facade of the agents' apartment is denoted by  $L_{\text{home}}$  and the average level resulting from the noise diary by  $L_{\text{diary}}$ .

## 4 Result

If the probability distribution in Fig. 5(a) or the probability density function of the average levels in Fig. 5(b) is considered, two distributions with different characteristics can be seen. The distribution of the levels at the apartment facades  $L_{\text{home}}$  is a bimodal distribution, where the lower maximum at 35–40 dB(A) with about 2250 agents is more pronounced than the upper maximum at 55–60 dB(A) with about 2000 agents. This bimodality can be explained by the location of the facade immission points. In the investigated area, the facade immission locations can be divided mainly into two categories. On the one hand there are facades, which are located directly at a street and on the other hand there are facades, which are located at the side of a building turned away from the street, for example in a backyard. Due to the attenuating effect of the obstacles, the road traffic noise level is self-explanatory significantly lower on the sides of the buildings facing away from the road. In the probability distribution of the average levels  $L_{\text{diary}}$  from the noise diaries this clear expression of two maxima is not to be seen. The upper maximum of the distribution here is also at 55–60 dB(A) but with 2800 agents it is much more pronounced than in the distribution of  $L_{\text{home}}$ . In the somewhat higher resolution probability density, a local maximum can be seen slightly above 35 dB(A), i.e. at the point where the probability density of  $L_{\text{home}}$  is maximum. However, this is not more pronounced than other local maxima between 45 and 50 dB(A), for example. A plateau is seen between 35 and 45 dB(A). It can be assumed that this is also a bimodal distribution, in which the lower maximum is much weaker than the higher one. Thus, by taking into account the location of the agents, there is a shift from lower averaging levels to higher averaging levels. This can also be seen in the mean values of the distributions.  $L_{\text{home}}$  has a mean value of 46.3 dB(A) and is thus 3.8 dB(A) lower than the mean value of  $L_{\text{diary}}$  with 50.1 dB(A). The medians of the two distributions differ slightly more than the mean, with a difference of 5.1 dB(A). The median of  $L_{\text{home}}$  is lower with 46.4 dB(A) than that of  $L_{\text{diary}}$  with 51.5 dB(A). Figure 6 (left) shows the pairs of values of the average levels  $L_{\text{diary}}$  over  $L_{\text{home}}$  from each agent in a scatter plot. Additionally, a red line is shown where the levels  $L_{\text{home}}$  and  $L_{\text{diary}}$  would be identical. It can be clearly seen that the scatter of the values depends on the value  $L_{\text{home}}$ . At lower levels, the largest distances to the red straight line above it are larger than the largest distances at higher levels. It is also clearly visible that the largest distances below the red straight line are smaller than the largest distances above the red straight line.

In Fig. 6 (right), the differences between  $L_{\text{diary}}$  and  $L_{\text{home}}$  over  $L_{\text{home}}$  are shown in a scatter plot for better illustration. Here, too, a red straight line is drawn at a difference of 0. In this diagram it can be seen that the maximum



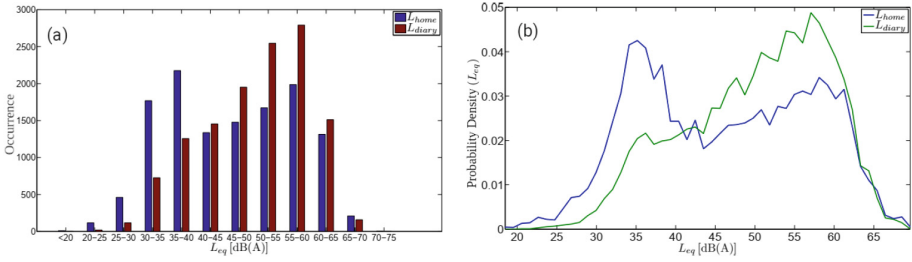


**Fig. 5.** (a) Occurrence distribution and (b) probability density function for the average sound level perceived by stationary ( $L_{home}$ ) and vagrant agents ( $L_{diary}$ ) in a span of a day.

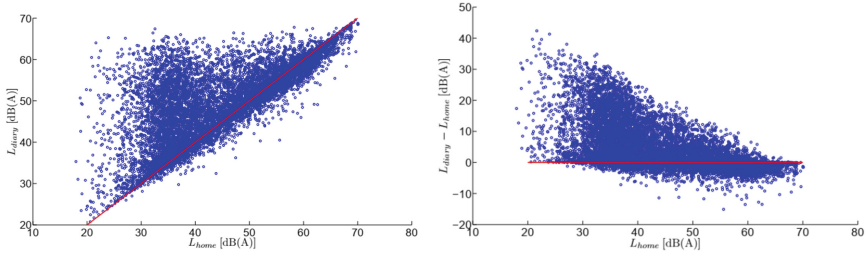


**Fig. 6.** (left) Scatter plot of the average level  $L_{diary}$  over the average level  $L_{home}$ . (right) Scatter plot of the differences of the averaging levels  $L_{diary}$  and  $L_{home}$  over the averaging level  $L_{home}$ . The values of the individual agents are represented by blue circles. The red line corresponds to a level difference of 0. (Color figure online)

magnification, i.e. values above the red straight line, falls with  $L_{home}$ . The maximum reduction, on the other hand, increases with  $L_{home}$ , but is much smaller in magnitude. The largest deviation into the positive range is about 42 dB(A), with the largest deviation into the negative range being about  $-15$  dB(A). The decrease of the deviations into the positive range with increasing  $L_{home}$  or the decrease of the deviations into the negative range with decreasing  $L_{home}$  can be easily explained. An agent has to move from one environment to a louder environment to increase the mean level. However, if the agent is already in a noisy environment, it is more likely to move to a quieter environment. Analogously, if agents are in a quiet environment. They would have to move to an even quieter environment to achieve a lower averaging level. Again, the opposite is more likely. Agents who are already in a quiet environment move more often to a louder environment than to an even quieter one. In this case, there are 7392 agents whose  $L_{diary}$  value is higher than the  $L_{home}$ . This corresponds to 58.96%. For two agents  $L_{home}$  and  $L_{diary}$  are identical, for the remaining 5144 agents, i.e. 41%,  $L_{diary}$  is lower than  $L_{home}$ . Since the maximum of the frequency distribution of  $L_{home}$  is at a relatively low level, it is plausible that more agents move to a noisier environment than to a quieter environment when considering



the daily schedule. The reason that the mean value of the  $L_{\text{home}}$  values is lower than the mean value of the  $L_{\text{diary}}$  values is on the one hand that more agents move into noisier environments, but on the other hand also that deviations into the positive difference range tend to be larger than deviations into the negative range. This fact can be well illustrated as in the following. If we imagine a quiet environment with an average level of  $L_1$  and a noisy environment with an average level of  $L_2$ , we can calculate an average level  $L_{eq}$ , which would result if an agent were to stay in the noisy environment for a duration of  $t_2$  and stay in the quiet environment for the rest of the observation time  $T$ , i.e.  $t_1 = T - t_2$ :

$$L_{eq}(t_2) = 10 \log_{10} \left[ \frac{1}{T} \left( (T - t_2) \cdot 10^{\frac{L_1}{10}} + t_2 \cdot 10^{\frac{L_2}{10}} \right) \right] \quad (2)$$

Figure 7 shows such a curve over one day, i.e.  $T = 24h$  with  $L_1 = 35$  dB(A) and  $L_2 = 60$  dB(A). Due to the logarithmic scale of the level, the increase of the average level with increasing duration of stay is greater for short durations of stay  $t_2$  than for longer durations of stay.

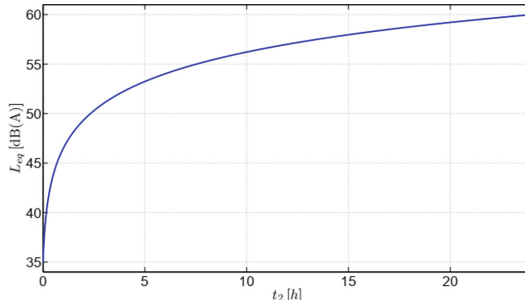


**Fig. 7.** Resulting average level over the time spent in a noisier area while staying in a quieter area for the rest of the day.

## 5 Conclusion

We conclude that the present combination of three state-of-the-art simulation tools allows us to account accurately for the noise level perceived by citizens in urban environments. We were able to reproduce the general trends in the noise-level distribution for stationary and vagrant agents and we quantified the impact on the exposure to road noise caused by traveling throughout the city or living in a road-side apartment. Further developments in this field could help to optimize the development of road networks and building blocks in urban environments which allow for a reduced noise pollution in critical areas and thus give rise to a higher overall quality of life.

## References

1. Fritschi, L., Brown, A.L., Kim, R., Schwela, D., Kephelopoulous, S.: Burden of Disease from Environmental Noise. World Health Organization, Bonn (2011)
2. Kwan, M.P.: *Int. J. Environ. Res. Public Health* **15**(9) (2018). <https://doi.org/10.3390/ijerph15091841>. <https://www.scopus.com/inward/record.uri?eid=2-s2.0-85052512806&doi=10.3390%2fijerph15091841&partnerID=40&md5=da530a4ed0152dc52b6d911a91db9d4c>. Cited by: 64; All Open Access, Gold Open Access, Green Open Access
3. Kang, T.S., Lee, L.K., Kang, S.C., Yoon, C.S., Park, D.U., Kim, R.H.: *J. Acoust. Soc. Am.* **134**(1), 822 (2013). <https://doi.org/10.1121/1.4807810>
4. Ma, J., Li, C., Kwan, M.P., Kou, L., Chai, Y.: *Environ. Int.* **139**, 105737 (2020). <https://doi.org/10.1016/j.envint.2020.105737>. <https://www.sciencedirect.com/science/article/pii/S0160412019318343>
5. Lu, M., Schmitz, O., de Hoogh, K., Hoek, G., Li, Q., Karssenber, D.: *Environ. Model. Softw.* **158**, 105555 (2022). <https://doi.org/10.1016/j.envsoft.2022.105555>. <https://www.sciencedirect.com/science/article/pii/S1364815222002559>
6. Park, Y.M., Kwan, M.P.: *Health Place* **43**, 85 (2017). <https://doi.org/10.1016/j.healthplace.2016.10.002>. <https://www.sciencedirect.com/science/article/pii/S1353829216304415>
7. Heinrichs, M.: Next Generation Forum 2011, ed. by P. Verkehr (Deutsches Zentrum für Luft und Raumfahrt e.V., 2011), pp. 74–74 (2011)
8. Lopez, P.A., et al.: The 21st IEEE International Conference on Intelligent Transportation Systems. IEEE (2018)
9. Kephelopoulous, S., Paviotti, M., Anfosso-Lédée, F.: Common Noise Assessment Methods in Europe (CNOSSOS-EU). Publications Office of the European Union (2012). <https://doi.org/10.2788/32029>